Int. J. Multiphase Flow Vol. 13, No. 4, pp. 535–547, 1987
Printed in Great Britain.

0301-9322/87 $3.00 + 0.00

SLURRY FLOW IN HORIZONTAL PIPES—EXPERIMENTAL AND MODELING

P. DORON, D. GRANICA and D. BARNEA
Department of Fluid Mechanics and Heat Transfer, Faculty of Engineering, Tel-Aviv University, Ramat-Aviv 69978, Israel

(*Received* 29 *October* 1986; *in revised form* 21 *January* 1987)

Abstract—The hydraulic transport of coarse particles in horizontal tubes has been investigated. A physical model for the prediction of the pressure drop and flow patterns is presented. The proposed model is compared with new experimental data and shows good agreement. Comparison with other proposed correlations is also satisfactory.

INTRODUCTION

The hydraulic transport of solid particles is a well-known method in the chemical and mining industries. In the case of coarse particle mixtures, settling effects are important, resulting in significant frictional losses and high pressure gradients.

Settling slurries exhibit a variety of flow patterns in horizontal pipeline flow. There is some diversity in the terminology which is used in the literature for the various flow patterns. However, the most common classification is: stationary bed, moving bed, heterogeneous suspension and pseudo-homogeneous suspension (Vocaldo & Charles 1972; Goedde 1978; Parzonka *et al.* 1981). There is also some confusion concerning the transition velocities between the flow patterns. In this work the velocity above which no stationary bed exists is termed the "deposit velocity", the velocity above which all the particles are suspended is the "suspending velocity" and the velocity above which the concentration profile is flat and the flow is homogeneous is called the "homogeneous velocity". The velocity which is associated with the minimum pressure drop is termed the "critical velocity".

The pressure drop is considered the most important parameter in slurry flow. The relationship between pressure gradient and mixture velocity is substantially different from that of a pure liquid flow. In contrast to single-phase flow where a monotonous behavior of the pressure drop curve is observed, the curve for slurry flow exhibits a minimum at the critical velocity.

Experimental data on the pressure gradient behavior of liquid–solid systems in horizontal pipes have been obtained by many investigators (Durand 1953; Zandi & Govatos 1967; Babcock 1971; Carleton *et al.* 1978; Chhabra & Richardson 1983; Noda *et al.* 1984). The prediction of pressure drop and flow patterns is a complex problem and is treated mostly via correlations of experimental data. Some of the empirical correlations claim to apply to all flow patterns for liquid–solid systems (Newitt *et al.* 1955; Hayden & Stelson 1971; Turian & Yuan 1977). Others are restricted to one or two flow patterns only (Durand 1953; Zandi & Govatos 1967; Babcock 1971; Toda *et al.* 1979; Wani *et al.* 1983; and many others).

Durand (1953) conducted experiments on sand–water and gravel–water flow at different particle and pipe sizes. He proposed the following empirical correlation for the pressure gradient:

$$\Phi = \frac{i - i_L}{C_s \cdot i_L} = K\left[\frac{U_s^2\sqrt{C_D}}{gD(s-1)}\right]^{-n}, \qquad [1]$$

where K and n are experimentally determined constants (K = 81, n = 1.5), i is the total pressure gradient (m_{water}/m), i_L is the pressure gradient for the carrier liquid flowing alone at the mixture superficial velocity, C_s is the slurry volumetric concentration, U_s is the slurry superficial velocity,

C_D is the drag coefficient for the solid particles, g is the gravitational acceleration, D is the pipe diameter and s is the solid-to-liquid density ratio.

Zandi & Govatos (1967) modified Durand's correlation by dividing its region of applicability into two parts, with different values of K and n for each of them.

Newitt *et al.* (1955) employed some theoretical considerations in order to identify the effective variables and obtained the following semi-theoretical expressions:

$$\left.\begin{aligned} \Phi &= 0.6(s-1), \quad \text{for pseudohomogeneous flow,} \\ \Phi &= 1100\frac{gDw}{U_s^3}(s-1), \quad \text{for heterogeneous flow,} \\ \Phi &= 66\frac{gD}{U_s^2}(s-1), \quad \text{for flow with a moving bed,} \end{aligned}\right\} \qquad [2]$$

where w is the terminal settling velocity of the solid particles.

The most comprehensive data bank was assembled by Turian & Yuan (1977). They used 2848 data points to develop a correlation whose form is

$$f_s - f_L = K_1 C_*^{K_2} f_L^{K_3} C_D^{K_4} \left[\frac{U_s}{gD(s-1)}\right]^{K_5}, \qquad [3]$$

where f_s and f_L are the friction coefficients for slurry flow and for pure liquid flow, respectively, C_* is the slurry volumetric concentration percent. The constants K_1–K_5 were determined for each of the four flow patterns by a best-fit procedure.

The theoretical prediction of pressure drop and flow patterns in slurry flow is quite complex. Some simplified physical models have been presented. Shook & Daniel (1965, 1969) and Shook *et al.* (1968) used a variable-density model to evaluate the effective friction coefficients for suspended flow and for flow with saltation. Their analysis requires prediction of the density distribution. This was indeed the subject of further research by Roco & Shook (1983, 1984, 1985) who analyzed the turbulent dispersion of the solid particles. Using some empirical coefficients, they offered a method to predict the velocity and concentration profiles for heterogeneous suspensions, as well as the deposit velocity. Carstens (1969) employed a diffusion equation in his analysis of flow with a stationary bed in order to estimate pressure drop curves. Wilson, in a series of papers (Wilson 1970, 1974, 1976; Wilson *et al.* 1972), reported an analysis which was based on a two-layer model in order to find the deposit velocity and the pressure drop for flow with a moving bed. Televantos *et al.* (1979) employed Wilson's two-layer model to analyze the pressure drop for flow with a moving bed. Thomas (1979a) analyzed the connection between the laminar–turbulent transition and the deposit velocity for highly viscous carrier fluid. Thomas (1979b) also proposed a theoretical approach for finding the deposit velocity for small particles. Oroskar & Turian (1980) employed energy conservation considerations to obtain an analytical expression for the suspending velocity. Support for this method when applied to fine particles is given by Shook *et al.* (1982). Toda *et al.* (1980) developed a theoretical model for the deposit velocity based on some saltation parameters. Later, Noda *et al.* (1984) used those parameters to develop an expression for the pressure drop for flow with saltation. Wani *et al.* (1983) suggested a simplified model for the pressure drop when the flow is fully suspended. However, they based it on an empirical correlation for the concentration gradient.

In this work an improved theoretical analysis is presented. Its purpose is to provide a method for predicting pressure drop and flow patterns for a wide range of flow conditions. The model is simple to use and gives reasonably accurate results. In addition new experimental data on pressure drop in horizontal slurry flow have been collected in our laboratory and compared with the proposed model.

ANALYSIS

Consider a solid–liquid mixture (slurry) containing settling particles flowing through a horizontal pipe. The solid particles are subjected to gravitational forces which tend to deposit them and to turbulent forces which tend to suspend them uniformly throughout the pipe cross section. At very

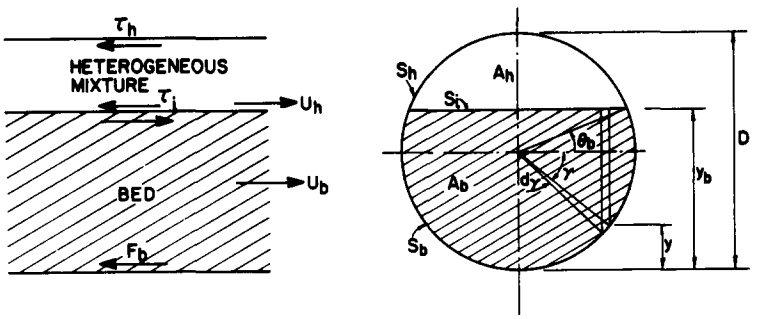

Figure 1. The two-layer model.

high mean slurry velocities the solid particles are almost symmetrically suspended, due to the high level of turbulence. Reduction of the mean velocity decreases the turbulent dispersing forces and causes a higher concentration of solid particles at the bottom of the pipe. As the mean velocity is decreased further, the particles may form a sliding deposit at the bottom, while the upper layer consists of a heterogeneous suspension. If the velocity is reduced still further the bed tends to become stationary.

Due to bed formation, the free passage cross-sectional area above the bed is narrowed, inducing an increase of the mean velocity in this region, and increasing the turbulent forces. The steady-state height of the bed is obtained when the velocity in the upper layer is sufficient to support all the particles that are still suspended. If the flow rate is increased, the magnitude of the dispersing forces increases, resulting in higher average concentration of particles in the upper layer and lower equilibrium bed height.

The process of analyzing the pressure drop behavior of slurry flow and the various flow patterns is based on a two-layer model. At very low mean mixture velocities it is assumed that either a stationary bed or a moving bed of solid particles is formed at the bottom of the pipe and a heterogeneous mixture of solid particles and carrier liquid is flowing at the upper part (see figure 1).

Assuming that the flow in each layer may be represented by means of the averaged properties (i.e. mean velocities and concentrations), and neglecting any slip between the two phases (i.e. considering the mean velocity of the solid particles as equal to the mean velocity of the liquid in each layer), the two continuity equations for a developed steady-state flow are:

$$U_h C_h A_h + U_b C_b A_b = U_s C_s A, \quad \text{for the solid phase;} \qquad [4]$$

and

$$U_h(1 - C_h)A_h + U_b(1 - C_b)A_b = U_s(1 - C_s)A, \quad \text{for the liquid phase;} \qquad [5]$$

where U is the mean velocity, C is the mean concentration and A is the cross-sectional area. The subscript h denotes the heterogeneous upper layer and b denotes the bed layer. U_s is the mixture velocity (i.e. the total slurry volumetric flow rate divided by A) and C_s is the slurry input concentration.

Force balances on each layer yield:

$$A_h \frac{dP}{dx} = -\tau_h S_h - \tau_i S_i, \quad \text{for the upper dispersed layer;} \qquad [6]$$

and

$$A_b \frac{dP}{dx} = -F_b + \tau_i S_i, \quad \text{for the bed layer;} \qquad [7]$$

where dP/dx is the pressure drop, τ_h and τ_i are the upper-layer shear stress and the interfacial shear stress acting on the perimeters S_h and S_i, respectively (see figure 1). F_b is the force acting on the bottom of the pipe and consists of two components: a dry friction force, F_{bd}, which is exerted by the bed particles on the surface of contact between the bed and the pipe wall, and a hydrodynamic resistance force, F_{bL}, which stems from the bed motion.

In the case of a stationary bed, F_{bd} is a static friction force and it balances the driving forces ($A_h\,dP/dx$ and $\tau_i S_i$) which act on the bed. When the driving forces are increased, the dry friction force increases, continuing to oppose them until its magnitude reaches a certain maximum value. At this state the bed is at the point of sliding and the friction force, F_{bd}, is equal to F_{bm}, which is calculated by $F_{bm} = \eta N$, where η is the dry friction coefficient and N is the sum of normal forces exerted by the solid particles in the bed on the pipe wall. For the case of a moving bed, $F_{bd} = F_{bm}$.

The normal forces, N, consist of two components, one which is due to the submerged weight of the solid particles, N_w, and an additional contribution due to the transmission of normal stresses which result from the shear on the bed–suspension interface, N_ϕ.

The calculation of the apparent weight component, N_w, is based on the assumption that the normal force exerted by the particles on the pipe wall can be represented by a pseudohydrostatic pressure distribution. This assumption has experimental verification (Wilson 1970) and is commonly used for slurry flows. Integration of this pressure distribution over the bed perimeter (figure 1) results in

$$N_w = 0.5(\rho_S - \rho_L)gC_bD^2\left[\left(\frac{2y_b}{D} - 1\right)\left(\theta_b + \frac{\pi}{2}\right) + \cos\theta_b\right], \qquad [8]$$

where ρ_S and ρ_L are the densities of the solid and the liquid, respectively.

The additional normal force N_ϕ is due to transmission of stress from the interface through the bed particles. Bagnold (1954, 1957) showed that when a fluid flows over a deposit of solid particles, there exists a normal stress at the interface which is associated with the shear stress exerted by the fluid on the bed. The relation is

$$N_\phi = \frac{\tau_i S_i}{\tan\phi}, \qquad [9]$$

where ϕ is the angle of internal friction. The value of $\tan\phi$ varies between 0.35 and 0.75 according to the type of flow and the particle characteristics.

Assuming that η is constant for a given solid, F_{bm} is evaluated by

$$\left.\begin{aligned} F_{bm} &= \eta(N_w + N_\phi), \\ F_{bm} &= \eta\left\{0.5(\rho_S - \rho_L)gC_bD^2\left[\left(\frac{2y_b}{D} - 1\right)\left(\theta_b + \frac{\pi}{2}\right) + \cos\theta_b\right] + \frac{\tau_i S_i}{\tan\phi}\right\}. \end{aligned}\right\} \qquad [10]$$

The hydrodynamic resistance force, F_{bL}, is due to the motion of the bed and is applicable only in the case of a moving bed. It may be expressed as follows:

$$F_{bL} = \tau_b S_b, \qquad [11]$$

where τ_b is the shear stress acting on the perimeter S_b (figure 1).

The hydrodynamic shear stresses τ_h and τ_b may be expressed by

$$\tau_h = \tfrac{1}{2} f_h \rho_h U_h^2 \quad \text{and} \quad \tau_b = \tfrac{1}{2} f_b \rho_b U_b^2. \qquad [12]$$

The friction coefficients are evaluated from

$$f_h = \alpha_h\left(\frac{\rho_h U_h D_h}{\mu_h}\right)^{-\beta_h} \quad \text{and} \quad f_b = \alpha_b\left(\frac{\rho_b U_b D_b}{\mu_b}\right)^{-\beta_b}, \qquad [13]$$

where ρ_h and ρ_b are the mean densities of the upper layer and of the bed, respectively, μ_h and μ_b are the mean viscosities of the two layers and D_h and D_b are the hydraulic diameters:

$$D_h = \frac{4A_h}{S_h + S_i} \quad \text{and} \quad D_b = \frac{4A_b}{S_h + S_i}. \qquad [14]$$

In this work the following coefficients were employed: $\alpha_h = \alpha_b = 0.046$, $\beta_h = \beta_b = 0.2$ for turbulent flow and $\alpha_h = \alpha_b = 16$, $\beta_h = \beta_b = 1.0$ for laminar flow. Note, however, that in this flow configuration, laminar flow in the upper layer is never encountered.

The interfacial shear stress, τ_i, is expressed in terms of the relative velocity between the two layers:

$$\tau_i = \tfrac{1}{2} f_i \rho_h (U_h - U_b)^2. \qquad [15]$$

The friction coefficient associated with the interface, f_i, is evaluated using the Colebrook (1939) formula with an interfacial effective roughness, which is assumed to be equal to the particle diameter. In order to account for the effect of suspended particles' collisions with the bed as well as entrainment and deposition of particles at the interface, which tend to increase the interfacial friction coefficient, Televantos *et al.* (1979) suggested multiplying the coefficient by 2, hence:

$$\frac{1}{\sqrt{2f_i}} = -0.86 \ln\left(\frac{\frac{d_p}{D_h}}{3.7} + \frac{2.51}{\mathrm{Re}_h\sqrt{2f_i}}\right). \quad [16]$$

The mixture mean properties are employed in evaluating the Reynolds numbers and the shear stresses. The densities are calculated by a weighted average which is commonly used in two-phase flow analysis:

$$\rho_h = \rho_S C_h + \rho_L(1 - C_h) \quad \text{and} \quad \rho_b = \rho_S C_b + \rho_L(1 - C_b). \quad [17]$$

The particles in the bed are in contact with each other. Therefore C_b is assumed to correspond to a maximum cubic packing of the deposited particles ($C_b = 0.52$). The viscosity of the mixture may be considered equal to that of the carrier liquid ($\mu_h = \mu_b = \mu_L$). This is due to the fact that the particles are coarse and larger than the scale of the viscous sublayer, hence they do not affect the apparent viscosity.

In addition to the conservation equations, the dispersion mechanism of the solid particles in the upper layer should be taken into account. This is assumed to be a turbulent diffusion process, which is governed by the large-scale eddies and tends to make the flow isotropic. Thus, it causes the motion of the solid particles from the high-concentration zone to the low-concentration zone, i.e. from the interface upward. This tendency is balanced at steady state by the gravitational effect which causes the particles to settle at the pipe bottom. This mechanism is represented by the well-known diffusion equation

$$\epsilon' \frac{\partial^2 C(y)}{\partial y^2} + w' \frac{\partial C(y)}{\partial y} = 0, \quad [18]$$

where $C(y)$ is the local volumetric concentration in the upper layer, y is the vertical coordinate (perpendicular to the pipe axis), ϵ' is the local diffusion coefficient and w' is the particles' local terminal settling velocity. A similar equation was presented by Okuda (1980). Assuming that the concentration depends only on the vertical position and that mean diffusion coefficient (ϵ) and terminal velocity (w) can be applied, [18] can be integrated twice to obtain the concentration distribution in the dispersed layer:

$$C(y) = C_b \exp\left[-\frac{w}{\epsilon}(y - y_b)\right]. \quad [19]$$

Note that the concentration at the interface in the dispersed layer is assumed to be equal to the bed concentration.

Assuming that the mass-transfer coefficient and the momentum-transfer coefficient are nearly equal, the mean cross-flow diffusion coefficient, ϵ, is evaluated according to Taylor (1954):

$$\epsilon = 0.052\, U_* r, \quad [20]$$

where $U_* = U_h\sqrt{f_i/2}$ is the shear velocity and r is the hydraulic radius of the upper-layer cross section.

The terminal settling velocity of a single particle, w_0, is evaluated from a force balance between the gravitational force and the drag force:

$$w_0 = \sqrt{\frac{4}{3}\frac{(s-1)d_p g}{C_D}}, \quad [21]$$

where C_D depends on the particle Reynolds number, $\mathrm{Re}_p = \rho_L w_0 d_p/\mu_L$. $C_D = 18.5\,\mathrm{Re}_p^{-0.6}$ for $0.1 < \mathrm{Re}_p < 500$ and $C_D = 0.44$ for $500 < \mathrm{Re}_p < 2 \times 10^5$ (Bird *et al.* 1960). For the settling of a

cluster of particles, the hindered terminal settling velocity, w, is found by the Richardson & Zaki (1954) correlation:

$$\frac{w}{w_0} = (1 - C)^m. \quad [22]$$

The parameter $m = 4.45\ \mathrm{Re}_w^{-0.1}$ for $1 < \mathrm{Re}_w < 500$ and 2.39 for $\mathrm{Re}_w > 500$, where Re_w is the particle Reynolds number based on w.

Integration of [19] yields the mean concentration in the upper dispersed layer, in terms of θ_b:

$$C_h = \frac{C_b D^2}{2A_h} \int_{\theta_b}^{\frac{\pi}{2}} \exp\left[-\frac{wD}{2\epsilon} (\sin\gamma - \sin\theta_b) \right] \cos^2\gamma \, d\gamma. \quad [23]$$

Final Formulation

The flow situation is therefore represented by a set of five equations:

$$U_h C_h A_h + U_b C_b A_b = U_s C_s A, \quad [24]$$

$$U_h(1 - C_h)A_h + U_b(1 - C_b)A_b = U_s(1 - C_s)A, \quad [25]$$

$$A_h \frac{dP}{dx} = -\tau_h S_h - \tau_i S_i, \quad [26]$$

$$A_b \frac{dP}{dx} = -F_{bd} - \tau_b S_b + \tau_i S_i \quad [27]$$

and

$$\frac{C_h}{C_b} = \frac{D^2}{2A_h} \int_{\theta_b}^{\frac{\pi}{2}} \exp\left[-\frac{wD}{2\epsilon} (\sin\gamma - \sin\theta_b) \right] \cos^2\gamma \, d\gamma. \quad [28]$$

Note that θ_b, A_h, A_b, S_h, S_i and S_b can all be expressed in terms of the bed height y_b (see figure 1).

Given any set of operational conditions and physical properties of the two phases, [24]–[28] can be solved for the following five state variables: U_h (the mean velocity in the dispersed layer), U_b (the mean velocity of the bed), C_h (the mean concentration in the dispersed layer), y_b (the bed height) and dP/dx (the pressure drop). In addition, the concentration profile in the upper heterogeneous layer, $C(y)$, can be found using [19] for any steady-state solution.

The mode of solution of the set of equations depends on the flow pattern.

Flow with a stationary bed

Let us start with a very low slurry superficial velocity, where a stationary bed is assumed. In this case the dry frictional force, F_{bd}, cannot be directly calculated from [10], since it applies only at the verge of motion. However, one equation can be eliminated, since by definition, the mean velocity of the bed is zero. Solution of [24] and [25] with $U_b = 0$, yields

$$C_h = C_s \quad \text{and} \quad U_h = U_s \frac{A}{A_h}. \quad [29]$$

Equation [28] can now be transformed into a single-variable equation for the bed height, y_b, since C_h is known and all the geometrical properties and other parameters can be expressed in terms of y_b.

Once the bed height has been found, all the geometrical properties as well as U_h and the shear stresses associated with the upper dispersed layer can be calculated. The pressure drop is then found using [26].

The static dry friction force, F_{bd}, can now be calculated from the momentum balance on the bed [27] and compared to the maximum dry friction, F_{bm}, which corresponds to the point of slip and is calculated from [10] for the same bed height y_b. The bed is indeed stationary as long as

$$F_{bd} < F_{bm}. \quad [30]$$

This condition was first presented by Wilson (1970).

As the slurry superficial velocity is increased, the shearing forces are increased while the bed height diminishes. A condition is reached when the resistance forces at the bed perimeter due to the dry friction (F_{bd}) are not sufficient to prevent the motion of the bed. At this point, $F_{bd} = F_{bm}$ and transition from a stationary to a moving bed occurs.

Flow with a moving bed

In this case the dry friction force component is a function of the bed height $[F_{bd} = F_{bm} = \eta(N_w + N_\phi)]$ and is calculated by [10]. However, no other variable may be estimated *a priori*. Therefore the whole set of five equations [24]–[28] has to be solved. The concentration profile in the upper dispersed layer can now be obtained using [19].

Fully suspended flow

As the slurry superficial velocity is further increased (for a given set of operational conditions), the bed height is reduced. When the bed height approaches zero, transition to fully suspended flow occurs. This transition may also occur directly from the stationary bed flow pattern. For this flow the pressure drop is calculated by

$$\frac{dP}{dx} = \frac{2}{D}\rho_M U_s^2 f_M, \qquad [31]$$

where $\rho_M = \rho_L(1 - C_s) + \rho_S C_s$ and f_M is calculated as in [13] with $U_h = U_s$ and $D_h = D$.

The vertical concentration profile is calculated using [19] with $y_b = 0$,

$$C(y) = C_B \exp\left(-\frac{w}{\epsilon} y\right). \qquad [32]$$

Note, that C_B (the concentration at the bottom of the pipe) is not equal in this case to the maximum packing concentration. However, it can be calculated using [28], since C_h is known to be equal to C_s. Substituting A_h by A and setting $\theta_b = (-\pi/2)$ in [28], yields

$$C_B = \frac{\pi}{2} C_s \int_{-\pi/2}^{\frac{\pi}{2}} \exp\left(-\frac{wD}{2\epsilon} \sin\gamma\right) \cdot \cos^2\gamma \, d\gamma. \qquad [33]$$

The local concentration at the top of the pipe, C_T, is obtained using [32] with $y = D$. As the slurry superficial velocity is increased, the value of ϵ also increases, and the ratio C_T/C_B approaches unity (i.e. the concentration profile flattens). The transition from heterogeneous to pseudohomogeneous flow is assumed to occur when the concentration distribution is essentially uniform, say, for example, $C_T/C_B \approx 0.95$. The pressure gradient for the pseudohomogeneous flow pattern is also evaluated using [31].

For any given set of operational conditions such as the pipe diameter, the slurry flow rate, the input solids concentration, the properties of the solid particles (density and diameter), the properties of the carrier liquid (density and viscosity) and the dry sliding friction coefficient, the flow pattern, pressure drop, bed height, mean velocities in the two layers and the concentration profile in the dispersed layer can be calculated. The critical velocity can also be evaluated by finding the minimum on the graph of pressure gradient vs slurry superficial velocity.

EXPERIMENTAL SYSTEM

A schematic layout of the experimental system is shown in figure 2. The system consists of a steel frame supporting the test section which is a transparent Plexiglas pipe, 11 m long, with an i.d. of 51 mm (2″) which is leveled to an accuracy of $\pm 0.1°$.

The slurry feed pipe is of Plexiglas with an i.d. of 40 mm (1.5″) that slopes downward at an angle of 2° to the inlet section (the feed pipe is always higher than the highest point of the test pipe).

The slurry is supplied from a 500 l. container, mixed by a 420 rpm mixer and circulates in a closed loop through the system by two slurry pumps with rubber-coated open impellers. The slurry flow rate can be controlled by a butterfly control valve and by bypass lines, and is measured by a slurry magnetic flow meter. In order to conveniently control the input concentration of the slurry a water

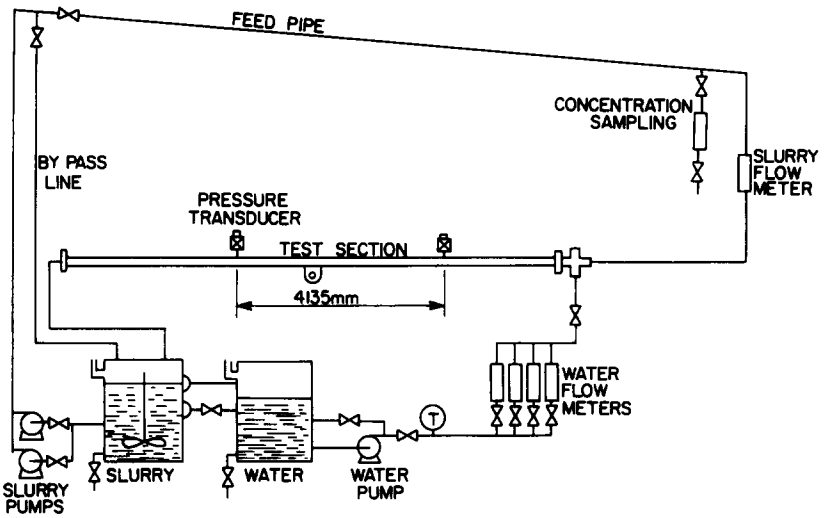

Figure 2. Experimental system.

loop can be added to the slurry loop. Concentration samplings are taken from the slurry supply line near the entrance to the test section.

The solid particles used are General Electric "Black Acetal" with a density of 1.24 gr/cm^3 and diameter of 3 mm.

The pressure drop in the test section is measured using two Validyne differential pressure transducers (DP15 and DP7) with direct connection to a digital computer for data acquisition and reduction. The flow patterns were determined by visual observation.

RESULTS AND DISCUSSION

Figure 3 shows the (dimensionless) pressure gradient, i, vs the mixture velocity for various input concentrations. The solid lines represent the theoretical results, and the (+) signs the data points.

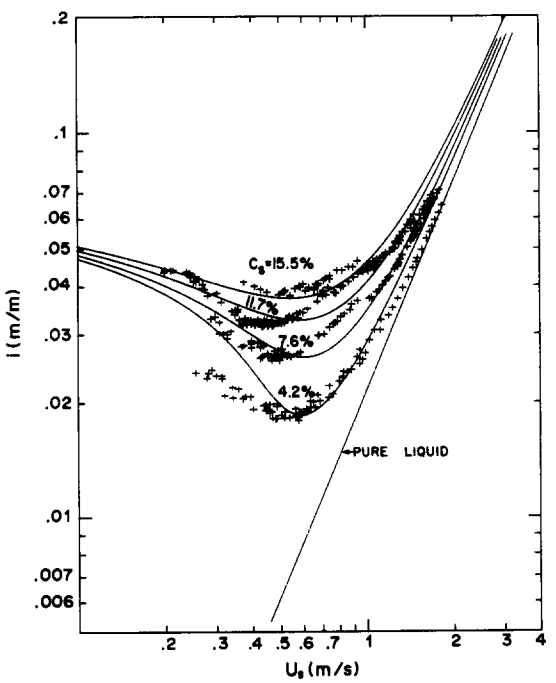

Figure 3. Comparison of the model results with experimental data—effect of slurry concentration. $\rho_s = 1240$ kg/m^3, $d_p = 3$ mm, $D = 50$ mm; +, experimental data; ——, theory ($\eta = 0.3$, $\tan\phi = 0.6$).

The results are typical of the pressure gradient behavior for slurry flow of coarse particles in horizontal pipes. At high superficial velocities, where the mixture is suspended, the slurry pressure drop is usually somewhat higher than that of the carrier liquid. Reduction of the mean velocity leads to bed formation and to pressure drops which are much higher than those of the pure liquid. The solid lines in the figure present the results of the theoretical model for the same conditions. The theory compares favorably with the experimental data. Increasing the input concentration results in higher pressure gradients, while the value of the critical velocity remains almost constant. This effect on both the pressure drop behavior and the critical velocity values is predicted quite accurately by the theoretical model. Almost all the experimental data were in the moving bed flow pattern. The theoretical model indeed predicts the moving bed flow pattern in the experimental velocity range.

Our experimental data and the theoretical model were also compared with previously published commonly used correlations for the prediction of pressure drop in slurry flow. Figures 4–7 show pressure drop curves for a given set of operational conditions which result from Durand's correlation [1], Zandi & Govatos' correlation, Newitt *et al.*'s method [2] and Turian & Yuan's correlation [3], as well as our experimental data and the theoretical prediction. Both the experimental data and the model predictions lie within the pressure drop range which is bounded by the other correlations. Moreover, the present experimental data compares better with the theoretical curves than with the other correlations. It should be noted that the best fit is observed between our results and Turian & Yuan's correlation, which is based on the largest data bank.

SPECIFIC ENERGY CONSUMPTION

An alternative way to represent the performance of hydraulic transport of solids is to plot the specific energy consumption against the solids throughput. This method was also presented by Streat (1982). This mode of presentation has practical significance. It is important to consider the energy requirement for the transportation of a given amount of solids, since it may be a dominant factor in the determination of the operation costs.

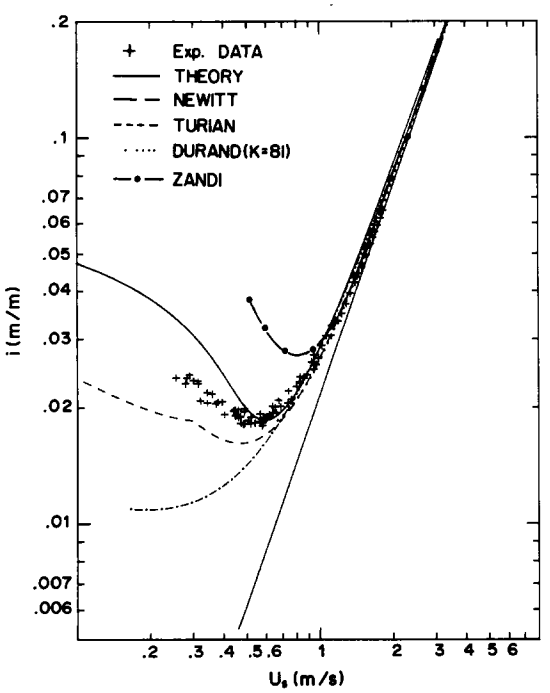

Figure 4. Pressure drop in slurry flow—comparison with published correlations. $\rho_L = 1000\ kg/m^3$, $\rho_S = 1240\ kg/m^3$, $d_p = 3\ mm$, $D = 50\ mm$, $\eta = 0.3$, $\tan\phi = 0.6$, $C_v = 4.2\%$.

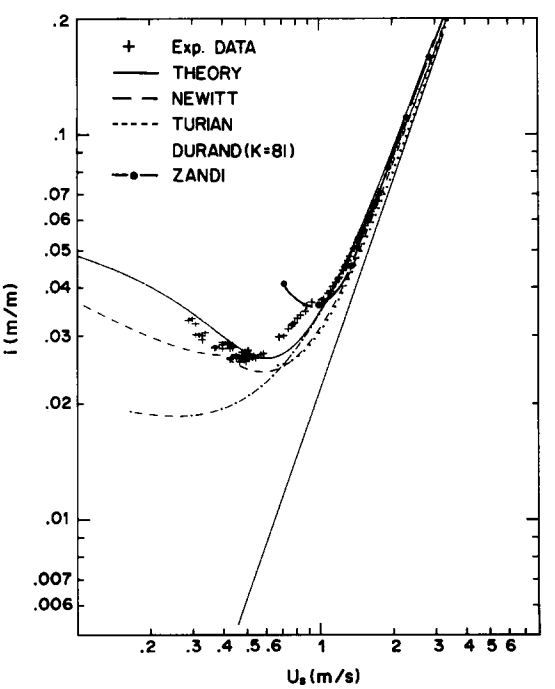

Figure 5. Pressure drop in slurry flow—comparison with published correlations. $\rho_L = 1000\ kg/m^3$, $\rho_S = 1240\ kg/m^3$, $d_p = 3\ mm$, $D = 50\ mm$, $\eta = 0.3$, $\tan\phi = 0.6$, $C_v = 7.6\%$.

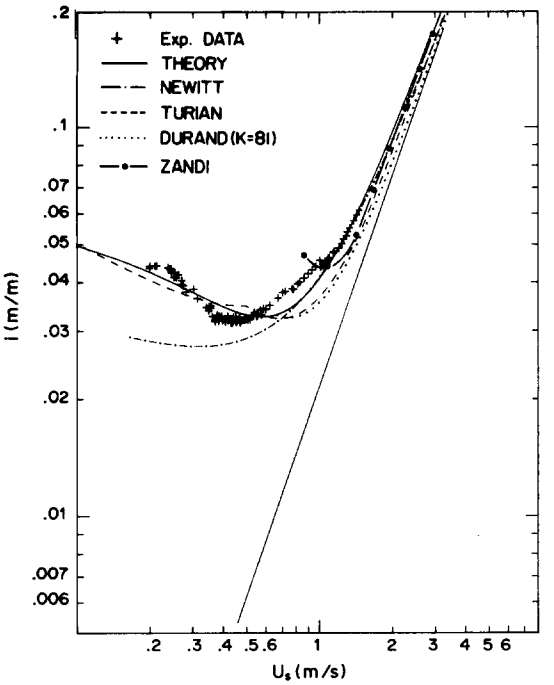

Figure 6. Pressure drop in slurry flow—comparison with published correlations. $\rho_L = 1000$ kg/m^3, $\rho_S = 1240$ kg/m^3, $d_p = 3$ mm, $D = 50$ mm, $\eta = 0.3$, $\tan\phi = 0.6$, $C_s = 11.7\%$.

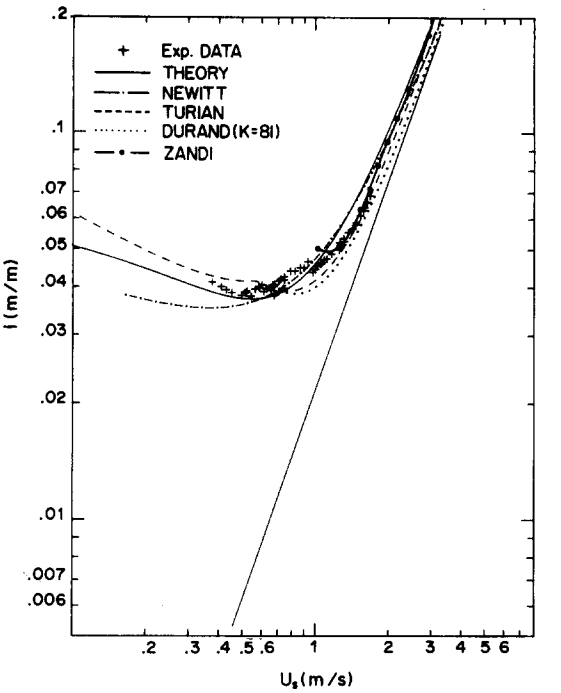

Figure 7. Pressure drop in slurry flow—comparison with published correlations. $\rho_L = 1000$ kg/m^3, $\rho_S = 1240$ kg/m^3, $d_p = 3$ mm, $D = 50$ mm, $\eta = 0.3$, $\tan\phi = 0.6$, $C_s = 15.5\%$.

The energy consumption per unit mass (of delivered solids) per unit length, E, is calculated by

$$E = \frac{dP}{dx}\frac{Q_s}{M_s}. \qquad [34]$$

For any slurry volumetric flow rate, Q_s, the pressure drop, dP/dx, is found by the method described before and the solids throughput, M_S, is calculated by

$$M_S = Q_s C_s \rho_S. \qquad [35]$$

The model results are shown in figure 8. An interesting behavior of the specific energy

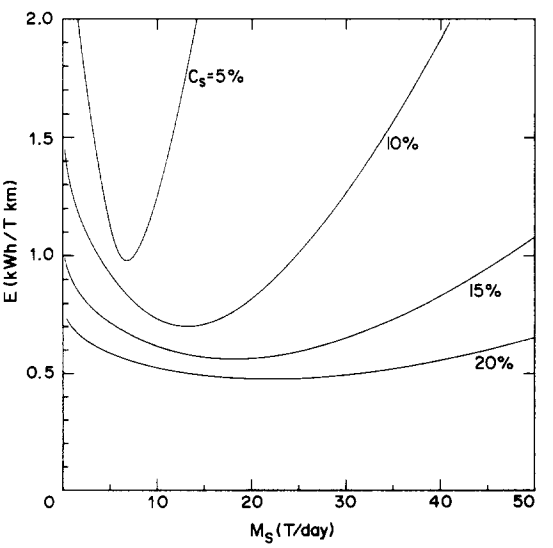

Figure 8. Effect of slurry concentration on specific energy consumption. $\rho_S = 1240$ kg/m^3, $D = 50$ mm, $d_p = 3$ mm, $\eta = 0.3$, $\tan\phi = 0.6$.

consumption curves is observed. Like the pressure gradient curves (figure 3), they display a minimum. However, their dependence on the slurry input concentration is quite different. While the pressure drop curves are shifted toward higher values when the concentration is increased, the specific energy consumption decreases. The reason for this behavior is that the slurry concentration has quite opposite effects on the solids throughput and on the pressure drop. As the concentration becomes larger, the solids throughput increases at a higher rate than the pressure drop. Moreover, in order to transport a given amount of solids, the slurry flow rate is reduced if the concentration is larger. The overall effect is a reduction of the specific energy which is required for the transportation of a given solids throughput. In particular, the minima of the curves are shifted toward higher throughput values and lower specific energy requirements for high solids concentrations. It should also be noted, that for the higher concentrations the curves on figure 8 flatten.

The combined effect of low specific energy consumption and its relative independence on M_S appear to point out that slurry transportation at high solids concentration is preferable. However, this is not the only factor that is to be considered. High concentrations are associated with the formation of high beds. Usually, it is desirable to avoid high beds, since they may cause enhanced pipe erosion as well as pipe blockage due to flow irregularities. In conclusion, the specific energy consumption should be considered together with the respective bed height in order to obtain the optimal conditions for the slurry transportation.

SUMMARY AND CONCLUSION

Solid–liquid slurry transportation has been investigated. New experimental data on pressure drop in horizontal slurry flow was collected. A theoretical model for the prediction of flow characteristics in solid–liquid flow was developed. The theory is based on a two-layer model. It allows the prediction of pressure drop and flow patterns once the slurry flow rate, input concentration, conduit geometry and solid–fluid properties are specified. The model predictions are compared to the new experimental data as well as to several widely used correlations.

Acknowledgement—The authors wish to thank the Bundsministerium für Forschung und Technologie (BMFT) for its support and Professor Dr Ing. Karl Stephan for his helpful cooperation.

REFERENCES

BABCOCK, H. A. 1971 Heterogeneous flow of heterogeneous solids. In *Advances in Solid Liquid Flow in Pipes and its Application* (Edited by ZANDI, I.), pp. 125–148. Pergamon Press, Oxford.

BAGNOLD, R. A. 1954 Experiments on a gravity-free dispersion of large solid spheres in a Newtonian fluid under shear. *Proc. R. Soc.* **A225**, 49–63.

BAGNOLD, R. A. 1957 The flow of cohesionless grains in fluids. *Phil. Trans. R. Soc.* **A249**, 235–297.

BIRD, R. B., STEWART, W. E. & LIGHTFOOT, E. N. 1960 *Transport Phenomena*, Chap. 6. Wiley, New York.

CARLETON, A. J., FRENCH, R. J., JAMES, J. G., BROAD, B. A. & STREAT, M. 1978 Hydraulic transport of large particles using conventional and high concentration conveying. In *Proc. 5th Int. Conf. on the Hydraulic Transport of Solids in Pipes*, Hanover, Paper D2, pp. 15–28.

CARSTENS, M. R. 1969 A theory for heterogeneous flow of solids in pipes. *Proc. ASCE, J. Hydraul. Div.* **95**(HY1), 275–286.

CHHABRA, R. P. & RICHARDSON, J. F. 1983 Hydraulic transport of coarse gravel particles in a smooth horizontal pipe. *Chem. Engng. Res. Des.* **61**, 313–317.

COLEBROOK, C. F. 1939 Turbulent flow in pipes with particular reference to the transition region between smooth and rough pipe laws. *J. Instn civ. Engrs* **11**, 133–156.

DURAND, R. 1953 Basic relationships of the transportation of solids in pipes—experimental research. In *Proc. 5th Minneapolis Int. Hydraulics Convent.*, Minneapolis, Minn., pp. 89–103.

GOEDDE, E. 1978 To the critical velocity of heterogeneous hydraulic transport. In *Proc. 5th Int. Conf. on the Hydraulic Transport of Solids in Pipes*, Hanover, Paper B4, pp. 81–98.

HAYDEN, J. W. & STELSON, T. E. 1971 Hydraulic conveyance of solids in pipes. In *Advances in Solid Liquid Flow and its Applications* (Edited by ZANDI, I.), pp. 149–163. Pergamon Press, Oxford.

NEWITT, D. M., RICHARDSON, J. F., ABBOTT, M. & TURTLE, R. B. 1955 Hydraulic conveying of solids in horizontal pipes. *Trans. Instn chem. Engrs* **33**, 93–113.

NODA, K., TAKAHASHI, H. & KAWASHIMA, T. 1984 Relation between behavior of particles and pressure loss in horizontal pipes. In *Proc. 9th Int. Conf. on the Hydraulic Transport of Solids in Pipes*, Rome, Paper D4, pp. 191–205.

OKUDA, K. 1980 Mechanism for suspension and dispersion for coarse solid particles in the hydraulic transport line. In *Proc. 7th Int. Conf. on the Hydraulic Transport of Solids in Pipes*, Sendai, Paper G3, pp. 291–300.

OROSKAR, A. R. & TURIAN, R. M. 1980 The critical velocity in pipeline flow of slurries. *AIChE Jl* **26**, 550–558.

PARZONKA, W., KENCHINGTON, J. M. & CHARLES, M. E. 1981 Hydrotransport of solids in horizontal pipes: effects of solids concentration and particle size on the deposit velocity. *Can. J. chem. Engng* **59**, 291–296.

RICHARDSON, J. F. & ZAKI, W. N. 1954 Sedimentation and fluidization, part I. *Trans. Instn chem. Engrs* **32**, 35–53.

ROCO, M. C. & SHOOK, C. A. 1983 Modeling of slurry flow: the effect of particle size. *Can. J. chem. Engng* **61**, 494–503.

ROCO, M. C. & SHOOK, C. A. 1984 A model for turbulent slurry flow. *J. Pipelines* **4**, 3–13.

ROCO, M. C. & SHOOK, C. A. 1985 Critical deposit velocity in slurry flow. *AIChE Jl* **31**, 1401–1404.

SHOOK, C. A. & DANIEL, S. M. 1965 Flow of suspensions of solids in pipelines, Part I. Flow with a stable stationary deposit. *Can. J. chem. Engng* **43**, 56–61.

SHOOK, C. A. & DANIEL, S. M. 1969 A variable-density model of the pipeline flow of suspensions. *Can. J. chem. Engng* **47**, 196–200.

SHOOK, C. A., DANIEL, S. M., SCOTT, J. A. & HOLGATE, J. P. 1968 Flow of suspensions in pipelines, Part II. Two mechanisms of particle suspensions. *Can. J. chem. Engng* **46**, 238–244.

SHOOK, C. A., GILLIES, R., HAAS, D. B., HUSBAND, W. H. W. & SMALL, M. 1982 Flow of coarse and fine sand slurries in pipelines. *J. Pipelines* **3**, 13–21.

STREAT, M. 1982 A comparison of specific energy consumption in dilute and dense-phase conveying of solid–water mixtures. In *Proc. 8th Int. Conf. on the Hydraulic Transport of Solids in Pipes*, Johannesburg, Paper B3, pp. 111–122.

TAYLOR, G. 1954 The dispersion of matter in turbulent flow through a pipe. *Proc. R. Soc.* **A223**, 446–468.

TELEVANTOS, Y., SHOOK, C. A., CARLETON, A. & STREAT, M. 1979 Flow of slurries of coarse particles at high solids concentrations. *Can. J. chem. Engng* **57**, 255–262.

THOMAS, A. D. 1979a Predicting the deposit velocity for horizontal turbulent pipe flow of slurries. *Int. J. Multiphase Flow* **5**, 113–129.

THOMAS, A. D. 1979b The role of laminar/turbulent transition in determining the critical deposit velocity and the operating pressure gradient for long distance slurry pipelines. In *Proc. 6th Int. Conf. on the Hydraulic Transport of Solids in Pipes*, Canterbury, Kent, Paper A2, pp. 13–26.

TODA, M., YONEHARA, J., KIMURA, T. & MAEDA, S. 1979 Transition velocities in horizontal solid–liquid two-phase flow. *Int. chem. Engng* **19**, 145–152.

TODA, M., KONNO, H. & SAITO, S. 1980 Simulation of limit-deposit velocity in horizontal liquid–solid flow. In *Proc. 7th Int. Conf. on the Hydraulic Transport of Solids in Pipes*, Sendai, Paper J2, pp. 347–358.

TURIAN, R. M. & YUAN, T. F. 1977 Flow of slurries in pipelines. *AIChE Jl* **23**, 232–243.

VOCALDO, J. J. & CHARLES, M. E. 1972 Prediction of pressure gradient for the horizontal turbulent flow of slurries. In *Proc. 2nd Int. Conf. on the Hydraulic Transport of Solids in Pipes*, Coventry, Paper C1, pp. 1–12.

WANI, G. A., MANI, B. P., SUBA RAO, D. & SARKAR, M. K. 1983 Studies on the hold-up and pressure gradient in hydraulic conveying of settling slurries through horizontal pipes. *J. Pipelines* **3**, 215–222.

WILSON, K. C. 1970 Slip point of beds in solid–liquid pipeline flow. *Proc. ASCE, J. Hydraul. Div.* **96(HY1)**, 1–12.

WILSON, K. C. 1974 Co-ordinates for the limit of deposition in pipeline flow. In *Proc. 3rd Int. Conf. on the Hydraulic Transport of Solids in Pipes*, Golden, Colo., Paper E1, pp. 1–13.

WILSON, K. C. 1976 A unified physically-based analysis of solid–liquid pipeline flow. In *Proc. 4th Int. Conf. on the Hydraulic Transport of Solids in Pipes*, Banff, Alberta, Paper A1, pp. 1–16.

WILSON, K. C., STREAT, M. & BANTIN, R. A. 1972 Slip–model correlation of dense two-phase flow. In *Proc. 2nd Int. Conf. on the Hydraulic Transport of Solids in Pipes*, Coventry, Paper B1, pp. 1–10.

ZANDI, I. & GOVATOS, G. 1967 Heterogeneous flow of solids in pipelines. *Proc. ASCE, J. Hydraul. Div.* **93**(HY3), 145–159.